REVIEW

Microstructure and Fractal Analysis of Fat Crystal Networks

Dongming Tang and Alejandro G. Marangoni*

Department of Food Science, University of Guelph, Guelph, Canada, N1G 2W1

ABSTRACT: This paper reviews the study of the morphology and physical properties of fat crystal networks. Various microscopical and rheological methods can be used to quantify the microstructure of fats, with the ultimate aim of relating structure to mechanical response. Even though a variety of physical models have been proposed to explain the relationship between the mechanical properties of fats and their microstructure, the fractal scaling model most closely describes the experimentally observed behavior. Mass fractal dimensions determined by microscopy and rheology can be used successfully to quantify the microstructure of fats since fractal dimension values are sensitive to the combined effects of crystal size, morphology, and the spatial distribution of mass within the fat crystal network. Methods used to determine the fractal dimension of a fat crystal network such as box counting, particle counting, Fourier transform, light scattering, and oil migration are explained in detail here. The relationship between fractal dimensions determined by microscopy and rheology are discussed in light of the fact that different measures of the fractal dimension describe different microstructural features in a fat crystal network.

Paper no. J11237 in *JAOCS 83*, 377–388 (May 2006).

KEY WORDS: Fats, fractal dimension, mechanical properties, microstructure, morphology, physical models.

In food products of high fat content, such as butter, margarine, and shortening, fat exists in a semisolid state, structured by an underlying fat crystal network (1–5). The physical properties of fat and food products containing fat are related to the structure of this fat crystal network (6–10). Like many other materials, fat crystal networks demonstrate distinct hierarchies of structural organization as shown in Figure 1 (11). Most of the studies on the structure and properties of fat crystal networks have concentrated mainly on lipid composition, polymorphism, and SFC (solid fat content). In general, few attempts have been made to establish relationships between the size, morphology, and mass distribution of fat crystals and the rheological properties of fats.

Most of the studies on the microstructure of fat crystal networks qualitatively describe the general trends of how processing conditions change the size and morphology of fat crystal clusters and the rheological properties of fat crystal networks. Many microscopy techniques, for example, PLM (polarized light microscopy) (9,11–16), SEM (scanning electron microscopy) (12,17–19), CSLM (confocal scanning light microscopy) (20), FFEM (freeze-fracture electron microscopy) (21,22), and cryo-SEM (23), have been used to visualize the microstructure of fat crystal networks. Although in these studies the relationship between the physical properties and the microstructure of fats was not studied quantitatively, these studies allow us to gain a deeper understanding of the structure of fat crystal networks and provide valuable data for further analysis.

In addition to microscopy, large- and small-deformation rheology has been used to probe the microstructure of fat crystal networks. Moreover, oil migration and light-scattering techniques have served the same purpose (21,24). As researchers gained a deeper understanding of the structure and properties of fat crystal networks, more realistic physical models were proposed. However, the quantitative study of the microstructure of fat crystal networks did not progress much until the introduction of the physical model of cross-linked fractal aggregates (3,8–10). In this model, a fat crystal network is considered to be composed of interconnected fractal fat crystal clusters. The fractal dimensions calculated by light scattering, rheology, and permeability approaches (termed here physical fractal dimensions) and image analysis of PLM images of fat crystal networks (termed here microscopy fractal dimensions) provide suitable parameters to describe quantitatively the spatial distribution of mass within fat crystal clusters as well as the network comprising many fat crystal clusters. The relationship between crystallization kinetics and the microstructure of fat crystal networks also has been quantitatively studied using the fractal concept (25).

In this paper, we will review studies on the microstructure of fat crystal networks and describe our fractal model. Methods used to determine microscopy and physical fractal dimensions of fat crystal networks are also explained in detail.

MORPHOLOGY OF FAT CRYSTALS

Qualitative study on morphology. The most popular method to visualize the microstructure of fat crystal networks is PLM. Because of their birefringence, fat crystals appear bright between two crossed polarized filters, while the liquid oil remains dark. For taking 2-D polarized light micrographs of a fat sample, a drop (about 10 μL) of melted fat (80°C) is placed on a heated glass slide and covered with a heated cover slip (80°C). The sample is then placed at the required temperature, or cooled at a certain rate, to induce crystallization. Polarized light images of the sample can be observed between two 90° crossed polarized filters without freezing or removal of the liquid oil.

*To whom correspondence should be addressed at Dept. of Food Science, University of Guelph, 50 Stone Road West, Guelph, Ontario, Canada, N1G 2W1. E-mail: amarango@uoguelph.ca

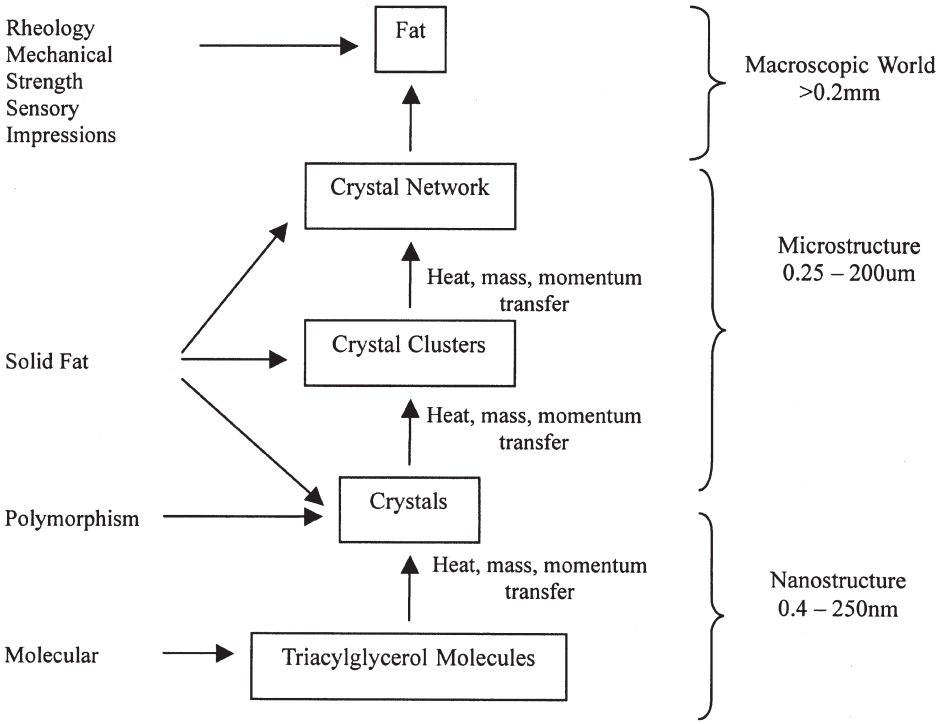

FIG. 1. Structure hierarchy of fat crystal networks (11).

Owing to the geometric restrictions of the 2-D space where crystallization takes place, the microstructure of the fat crystal networks observed using PLM of fat thin films may be different from that of bulk fat samples. Some attempts have been made to study the microstructure of fat crystal networks in 3-D space. Litwinenko (26) took polarized light micrographs of fat samples with thicknesses of 207 μm. 2-D polarized light micrographs of the sample at different depths were taken and converted into a 3-D view of the fat crystal network after deconvolution and a 3-D volume rendering. But this method only works for fat samples with low SFC. When the SFC of fat samples is high, it is difficult to take a polarized light micrograph of the thick fat samples.

In addition to the PLM method, EM (electron microscopy) has been used to study the microstructure of fat crystal networks (12,17,18,21,27). Most of the EM performed on fats has been freeze-fracture SEM, which does not require the electron beam to pass through the sample. Thus, it can be used to visualize the surface microstructure of thick fat samples at high SFC. The problem with the freeze-fracture SEM technique is the removal of the liquid oil entrapped within the fat crystal network to improve the visualization of the fat crystals. One of the most successful SEM methods was developed by Heertje *et al.* (17). They designed a special sample holder and used a mixture of 2-butanol and methanol (90:10, vol/vol) as a solvent to de-oil margarine samples containing as much as 80% liquid oil. The scanning electron micrograph of the fat crystal networks was taken after removing the liquid oil, with a resolution of ~1 μm. In addition to SEM, CSLM and FFEM have been used to study the microstructure of fatty products such as shortening, margarine, and butter (12,20–23). SEM images can provide information about the surface of the fat, whereas PLM images of fat samples provide a cross-sectional, or internal structural view of the sample (18). In recent years, PLM has gained more popularity than the SEM techniques because PLM can provide sharper images and sample preparation is easier.

By using these microscopy techniques, the morphology of the fat crystal clusters can be studied. Much information on how the shape and size of the fat crystal clusters change with different temperatures, polymorphism, chemical composition, and SFC is available (2,3,12,13,17,20,21,23,28,29). The shape of the fat crystal clusters can be spherulitic, feather-like, blade- or needle-shaped. The size of fat crystal clusters can vary from several micrometers to more than 200 μm.

In addition to their effects on the shape of fat crystal clusters, processing conditions can affect the size of the fat crystal clusters. Many studies have shown that an increasing crystallization temperature, a decreasing cooling rate and agitation rate all lead to an increases in crystal size (14,20,29).

The effects of processing conditions, especially the effects of crystallization temperature on crystal size, have been explained by different nucleation rates brought about by different processing conditions (30): At high crystallization temperatures, or slow cooling rates, the nucleation rate decreases. Because a decreased nucleation is usually accompanied by a relative increase in crystal growth (20), it is not surprising to discover crystal size increases at higher crystallization temperatures and/or slow cooling rates.

Another interesting area of scientific and technological en-

deavor is the study of the effects of shear on fat structure. Mazzanti *et al*. (31) have shown the shear-induced orientational effects on fat crystals from their nonisotropic 2-D X-ray diffraction patterns. The orientational effects induced by shear have been explained as being a consequence of the asymmetry in fat crystal growth induced by the shear fields that overcome Brownian thermal effects. Mazzanti *et al*. also reported that shearing can accelerate the transformation of fat crystals to more stable polymorphs. Moreover, a kinetic model for phase transition kinetics during the crystallization of a multicomponent fat under shear was given (32).

In general, the shape and size of fat crystal clusters are dependent on processing conditions and SFC and are less dependent on the final polymorphism of the fat crystals. In other words, fat samples with the same final polymorphism can have fat crystal clusters with different shapes and sizes depending on processing conditions and SFC.

This effect was shown by Manning and Dimick (18). The morphology of cocoa butter samples with different polymorphism was studied by SEM and PLM. Fat crystal clusters with irregular, spine-like, feathery, and needle-like shapes were found for the β and β′ forms depending on the crystallization temperature and the incubation time. Failey *et al*. (33) also showed that the morphology of blends of butter fat and tripalmitin was strongly dependent on the blending ratio and less dependent on the polymorphic form of the fat crystals. Herrera and Hartel (34) cooled different blends of HMF (high-melting fraction of milk fat) in LMF (low-melting fraction of milk fat) at 0.2 and 5.5°C/min to different temperatures and observed different fat crystal sizes and morphology, although the same β′ polymorph was present in all samples.

The importance of crystallization rate and SFC and the lesser importance of final polymorphism on the morphology of the fat crystal clusters confirm that a structural hierarchy exists within fat crystal networks. Polymorphism has to do with different molecular packing arrangements of TAG molecules, at the nanostructural range, within the primary fat crystals. Once the primary fat crystals are formed, they aggregate, or grow into each other, to form fat crystal clusters, which in turn cross-link to build up a 3-D fat crystal network. Microscopy is sensitive to the microstructural level of structure in fat crystal networks and to the morphology of fat crystal clusters, which is controlled by the kinetics of primary crystal aggregation/nucleation.

Quantitative study on the morphology and fractal dimensions of fat crystal networks. Because fat crystal clusters are usually shaped irregularly and their sizes are heterogeneous, it is not easy to quantify their structure, nor to build a numerical relationship between the morphology of the fat crystal clusters and their physical properties. Moreover, since manually measuring the crystal size, morphology, and spatial distribution was too tedious, few attempts to quantify the microstructure of fat crystal networks were made until image analysis software became widely available. Herrera and Hartel (34) studied fat crystal size distribution of blends of HMF in LMF, with blending ratios ranging from 30% HMF to 50% HMF, by cooling samples at 0.2 and 5.5°C/min to 25 and 30°C with or without shear. The results clearly showed that, on increasing the HMF ratio from 30 to 40%, the diameter of fat crystal clusters became smaller. For the same 50% HMF, the diameter of the fat crystal clusters increased from 200–280 μm to 360–520 μm when the crystallization temperature increased from 25 to 30°C and decreased to 80–140 μm when the shear rate was increased from 50 to 200 rpm. The selection of the parameter used to quantify the fat crystal clusters' size must be done carefully. For example, although different cooling rates result in fat crystal clusters with different size distributions, their average crystal size hardly varied in some experiments (35). Other parameters such as the median volume diameter, which corresponds to the 50th percentile of the particle volume frequency curve, and the modal volume diameter, which corresponds to the peak of the volume frequency distribution, may be better parameters to quantify fat crystal cluster size (36).

The concept of a fractal dimension was first introduced by Benoit Mandelbrot (37). The idea is to use a fractal number to describe the self-similar or self-affine character of some objects quantitatively. Fractal geometry provides a new paradigm to understand many physical phenomena. The fractal nature of fat crystal networks was first recognized by Vreeker *et al*. (8) and further explored by our research group. Fractal dimensions calculated by microscopy methods such as box counting, particle counting, and Fourier transforms of polarized light micrographs of fats can be used to quantify the microstructure of fat crystal networks. The fractal dimensions describe the combined effects of morphology and spatial distribution patterns of the crystal clusters in fat crystal networks.

Fractal dimension by microscopy methods. In general, fractal dimensions by microscopy methods provide a description of how space is occupied by a particular curve or shape. A fractal dimension is an intensive property of an object (38) and is used to quantify the variation in length, area, volume, or other properties with changes in the scale of the measurement interval. To calculate the fractal dimensions of an object, a property of the fractal object such as length L, is measured at different length scales r. For a self-similar fractal object, the length L displays a power law relationship to the length scale r, and the fractal dimension of the object can be derived from the exponential term. This principle is applied to calculate the box-counting, particle-counting, and Fourier transform fractal dimensions. The only differences among these methods are the properties measured and the formula used to calculate the fractal dimensions from the exponential term.

Box-counting fractal dimension, D_b. To calculate the box-counting fractal dimension, grids with side length l_i are laid over the polarized light micrographs of fat crystal networks. Any grid containing particles of more than a threshold value is considered to be an occupied grid. The number of occupied grids N_i for side length l_i is counted. This process is repeated for grids with different side lengths. The box-counting fractal dimension, D_b, is calculated as the negative of the slope of the linear regression curve of the log-log plot of the number of occupied boxes N_b vs. the side length l_b:

$$D_b = -\frac{\Delta \ln N_b}{\Delta \ln l_b} \quad [1]$$

To reduce errors and artifacts, small and large box sizes should be exempted from the calculation (39).

Particle-counting fractal dimension, D_f. The concept of particle-counting fractal dimension D_f is derived from the mass fractal dimension D_m, where D_m relates the number of particles N to the linear size of the fractal object R, and the linear size of one particle (microstructure element) a as:

$$N = \left(\frac{R}{a}\right)^{D_m} \qquad N >> 1 \quad [2]$$

If the average size of the microstructural element is assumed to remain constant (9), then Equation 2 becomes:

$$N \propto R^{D_f} \quad [3]$$

where D_f is the particle-counting fractal dimension. To calculate the value of D_f, 2-D polarized light micrographs of fat crystal networks are used. The logarithm of the number of microstructure elements $\log(N(R))$ is plotted against $\log R$ for varying values of R. The slope of the linear regression curve is the particle-counting fractal dimension D_f (9). The particle-counting fractal dimension algorithm should be carried out within the range between 100 and 35% of the original image size (5).

Fractal dimension by Fourier transform method, D_{FT}. In image analysis, a 2-D image is considered to be a discrete function, $f(x,y)$, where x and y are the coordinates of the object pixels in the horizontal and vertical direction. The 2-D discrete Fourier transform is applied to transform a 2-D image to its corresponding frequency domain image $F(u,v)$ as:

$$F(u,v) = \frac{1}{MN}\sum_{x=0}^{M-1}\sum_{y=0}^{N-1} f(x,y) * e^{-j*2\pi(ux/M+vy/N)} \quad [4]$$

or, expressing it in the form of sine and cosine functions, as:

$$F(u,v) = \frac{1}{MN}\sum_{x=0}^{M-1}\sum_{y=0}^{N-1} f(x,y)[\cos(2\pi(ux/M+vy/N)) - j\sin(2\pi(ux/M+vy/N))] \quad [5]$$

where u and v are the coordinates of the pixels in the frequency domain image. The power spectrum of $F(u,v)$, is

$$P(u,v) = |F(u,v)|^2 = R^2(u,v) + I^2(u,v) \quad [6]$$

where $R(u,v)$ is the real part of the function $F(u,v)$ and $I(u,v)$ is the imaginary part.

The frequency domain image is the transformed plotting of $P(u,v)$ against u, v dimension.

Since a fractal profile by definition includes information at all frequencies, calculating fractal dimensions from frequency domain images might seem to be difficult. In fact, the formula used to calculate fractal dimensions from the frequency domain image is simple. The logarithm of the magnitude, which is the square root of the power spectrum in the frequency domain image, shows a linear relationship with the logarithm of the frequencies. The slope of this linear relationship, β, is related to the fractal dimension D_{FT} as: $D_{FT} = (4 + \beta)/2$ (40). D_{FT} can be used to study both self-similar and self-affine fractal objects. The data at low frequencies (u and v <10) are not to be included in the calculation of D_{FT} (40). Figure 2 illustrates how D_b, D_f, and D_{FT} are calculated from polarized light micrographs of fat crystal networks.

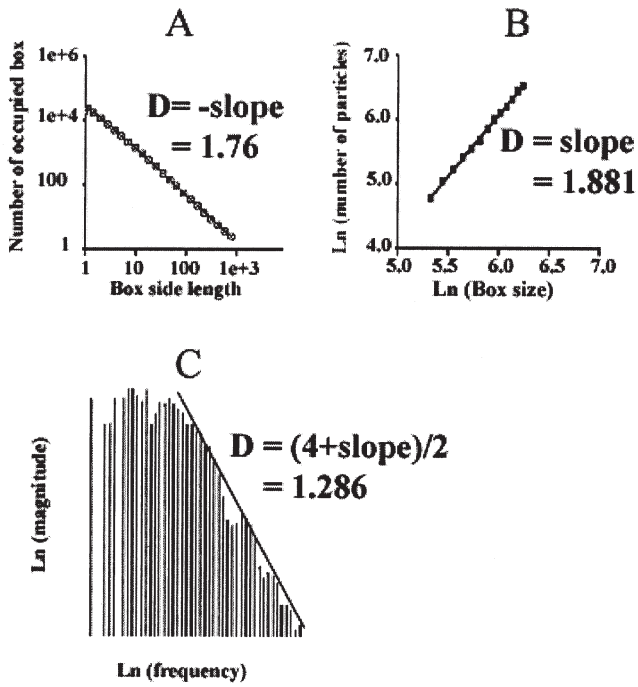

FIG. 2. Illustration of the log-log plot between (A) the number of occupied boxes with box size to calculate D_b, the box-counting fractal dimension; (B) the number of fat crystals inside each ROI (region of interest) with ROI size; and (C) magnitude and the frequency of the power spectrum image obtained by 2-D Fourier-transformation of the polarized light microscopy of fat crystal networks (41).

The general scheme for determining the microscopy fractal dimensions is shown in Figure 3. One small drop of melted fat sample (about 10 μL) is placed on a glass slide and then covered using a cover slip. The sample is kept above its melting temperature for a certain period of time to remove any crystal memory effects, then cooled, and the structure of the fat samples is imaged using PLM. To determine the box-counting and particle-counting fractal dimensions, the polarized light micrographs of the fat samples need to be thresholded to binary images, and then a commercial available software, Benoit 1.3 (TruSoft International, Inc., St. Petersburg, FL), and a self-written program, particleCounting.m (41), are used to calculate the D_b and D_f separately. Care must be taken in the selection of the threshold value. Because the global threshold method is applied by most of the commercial image analysis softwares, it is important to obtain a well-balanced illuminated image prior to thresholding. Other common practices to obtain high-quality PLM images include a background subtraction, where an image of the background liquid oil is taken and then subtracted from the images of the fat crystal networks, and frame averaging, where several images of

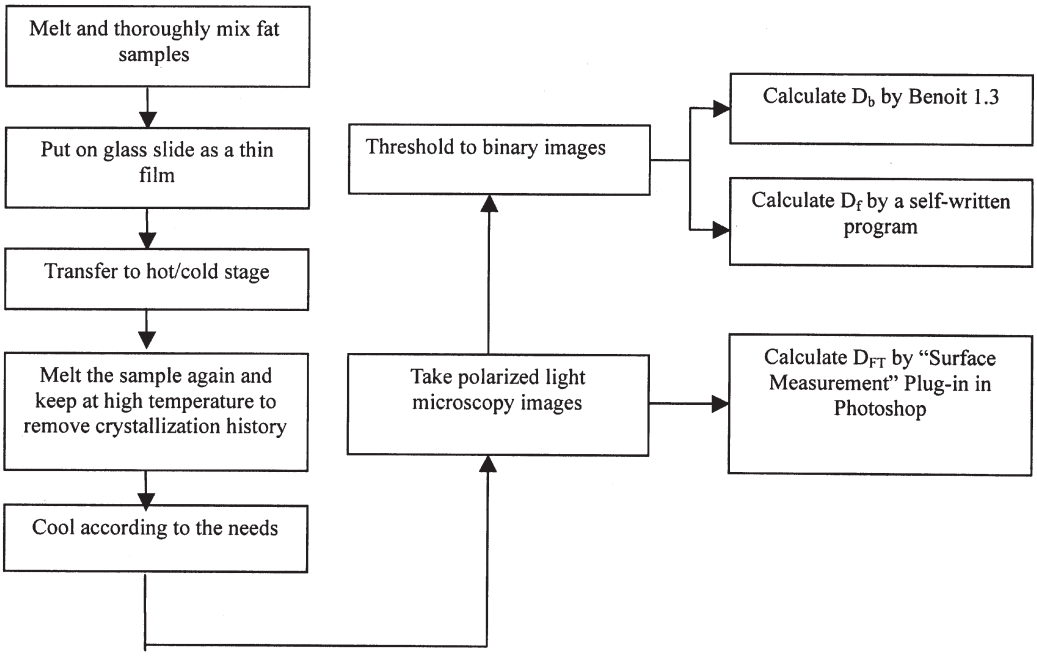

FIG. 3. General scheme to measure microscopy fractal dimensions of fat crystal networks. D_b, box-counting fractal dimension; D_f, particle-counting fractal dimension; D_{FT}, fractal dimension by Fourier transform method; Benoit 1.3 (TruSoft International, Inc., St. Petersburg, FL).

the same sample area are taken and then averaged to remove the noise. In contrast to D_b and D_f, the fractal dimension by Fourier transform method, D_{FT}, can be determined directly from the grayscale images. To measure D_{FT}, the grayscale polarized light micrographs are transformed from a spatial domain to a frequency domain by applying a 2-D discrete Fourier transformation. The D_{FT} can be calculated from the slope of the log-log plot of the magnitude against the frequency of the frequency domain image. All these manipulations can be done using Photoshop (Adobe, San Jose, CA) plug-ins.

All current microscopy fractal dimensions are derived from 2-D polarized light micrographs, so they are 2-D fractal dimensions. According to the commonly used method, fractal dimensions of fat crystal networks in 3-D space can be obtained by adding "1" to the 2-D fractal dimensions (40).

Fractal dimensions have been used extensively to quantitatively describe the microstructure of fat crystal networks (8–10,12,26,39,42–47). Awad *et al.* (13) measured the box-counting fractal dimension, D_b, of AMF (anhydrous milk fat), PO (palm oil), and CB (cocoa butter). The D_b of all the fat samples were found to increase with SFC up to a critical SFC value where they reached a plateau. The trends in D_b of the samples correspond well with their polarized light micrographs: The lower D_b values correspond to larger microstructures at low SFC, whereas higher D_b values correspond to a large number of smaller microstructures at high SFC. When the SFC of the fat samples was above a critical point, fat crystals filled space homogeneously on the microscope slide, and the D_b of the samples could not increase any further. For thick fat samples, the fractal dimensions of the fat crystal network D_b and D_f had their highest values at an intermediate depth (26).

The fractal dimensions calculated by different methods may have different values for the same fat crystal networks (40) and even display different trends when the microstructure of the fat crystal networks is changed (40,48). Through computer simulation, Tang and Marangoni (41) found that, in general, D_f reflects the radial mass density spatial distribution in the fat crystal networks whereas D_{FT} is more sensitive to cluster size and morphology and D_b is affected by SFC, cluster size, and crystal morphology. For example, for 20% SFC and diamond-shaped crystals, the D_b of the fat crystal network increased from 1.44 to 1.58 when the radius of the crystals was increased from 3 pixels to 42 pixels. In contrast, for 20% SFC, as the radius of the crystals was increased from 2 pixels to 6 pixels, D_{FT} decreased from 1.748 to 1.45. By comparing the affecting factors of D_b, D_f, D_{FT}, the particle-counting fractal dimension, D_f, and the Fourier-transform fractal dimension, D_{FT}, were found to be better parameters to represent the microstructure of the fat crystal networks than the box-counting fractal dimension, D_b.

MICROSTRUCTURE OF FAT CRYSTAL NETWORKS AND CRYSTALLIZATION KINETICS

The usefulness in the quantification of the microstructure of fats using the concept of fractal dimension arises from the possibility of relating structure to physical properties. Crystallization kinetics profoundly influences the final structure of fats, thus it would be useful if a quantitative relationship existed between them.

The relationship between crystallization kinetics and the microstructure of fat crystal networks was first proposed by our group in a study on the crystallization and structure of cocoa butter (42). The D_b of the polarized light micrographs of cocoa butter were found to be a function of the natural logarithm of the nucleation rate J, i.e. ,

$$D - D^* = \beta \ln J \quad [7]$$

where D is the D_b of cocoa butter, D^* is the D_b of a microstructure arising from a crystallization process with a nucleation rate of unity ($J = 1$), and β is the slope of the linear regression curve between D and ln J. From the Fisher–Turnbull equation we know that

$$\ln J = \alpha - \frac{\Delta G_n}{k_B T} \quad [8]$$

where α is a variable depending on temperature and the free energy of diffusion, ΔG_n is the free energy of nucleation, k_B is the Boltzmann's constant (J mol^{-1} K^{-1}), and T is the absolute temperature. Replacing ln J in Equation 7 by Equation 8, we obtain:

$$D - D^* = \alpha\beta - \beta\frac{\Delta G_n}{k_B T} \quad [9]$$

This suggests that the change in nucleation free energy results in a change in the D_b of the polarized light micrographs of fat crystal networks. By using fractal geometry concepts, it is possible to define the meaning of the above parameters (43).

This work links the microstructure of fat crystal networks with their crystallization kinetics, thus building a physical basis for the fractal nature of fat crystal networks. Although the relationship between the fractal nature of a cluster with aggregation kinetics of the particles was shown by computer simulation (49,50), little work has been done on the microstructure of fractal networks and its relationship with crystallization or aggregation kinetics. It would be interesting to apply our findings and simulate how the microstructure of fat crystal networks changes with varying nucleation free energies and temperature based on Equation 9.

PHYSICAL PROPERTIES OF FAT CRYSTAL NETWORKS

Fat-structured products contain a fat crystal network formed by solid fat crystal clusters and liquid oil entrapped within. These materials are viscoelastic, which means they display both viscous and elastic properties. Many methods have been used to characterize the mechanical properties of fat samples including large-deformation and small-deformation (rheological) tests.

In large-deformation tests, the bulk fat products are considered as a plastic material, which is elastic when the stress (or strain) is below the yield stress (or strain) and is viscous when the stress (or strain) is above the yield stress (or strain). The elastic properties of the plastic fats are modeled as $\tau = G\gamma$, and its viscous properties above the yield stress are modeled as $\tau - \tau_0 = \eta\ (d\gamma/dt)$, where τ is the stress, τ_0 is the yield stress, G is the elastic modulus, η is the viscosity, γ is the strain, and t is the time. During a large deformation test, the sample is deformed until it reaches its critical point and a permanent deformation or fracture is induced. The stress and strain during this deformation are measured, and information about the yield stress and elastic modulus is obtained. To describe the behavior of such materials, the yield stress and the relationship between the stress and strain below the yield stress must be determined.

The penetrometry method is a large-deformation test and is widely used to determine the yield stress or the firmness of a plastic fat (AOCS method Cc 16-60; 51). During the penetrometry test, the penetrating object geometry (could be a cone, a needle, or a plate) is held in contact with the surface of the sample and then is released. The time required to reach a particular depth is recorded. The yield stress can be calculated from the mass, the angle of the geometry, and the penetration depth after a predetermined period of time according to the equation $Y = CM/P^n$ (7,52–55), where Y is the yield stress, M is the mass of the penetrating objectgeometry, P is the penetrating depth, n is a constant, and C is a constant that depends on the geometry of the cone. The hardness index (HI) of the material is given by HI = M/P, where P is within the range of 1.5–5 mm (56).

In addition to the penetrometry method, the two-plate compression method is also used to study the structure of fats. A uniaxial parallel force is applied to fat samples, which are held between two parallel plates, to determine the yield force of the samples. The compression experiment can be combined with creep tests, in which a constant load is applied to the sample and the change in the deformation of the samples over time is monitored, or carried out in a constant speed mode, where the top plate moves down to the top surface of the fat sample at a constant speed.

The large-deformation method has been widely used to study the physical properties of fat products, such as the spreadability of shortenings and the hardness of chocolate and milk fat, and the results have been found to correlate well with sensory tests (14,56–58).

Although large-deformation tests for some fat samples correspond well with their sensory tests' results, it is difficult to relate the result from large-deformation experiments to any fundamental characteristics of the microstructure of fat crystal networks since the structure of the fat crystal networks is destroyed during the test. Small-deformation experiments have thus gained popularity in the study of the microstructure of fat crystal networks.

A small-deformation test refers to the rheological experiment in which the deformation of the fat samples is within the LVR (linear viscoelastic region, where the strain is proportional to the applied stress) of the fat samples. The fat samples are considered to be viscoelastic materials at small deformations. Viscoelastic fat products demonstrate elastic and viscous properties, so the shear modulus G consists of two components: the storage shear modulus G' and the loss shear modulus G''. The G' is the solid-like property of the fat samples, more specifically, the strength of the links between the fat crystal clusters, whereas G'' is the liquid-like property of the fat samples. A dy-

namic controlled strain or stress test is used to determine the moduli of the fat samples, where the samples are subjected to a sinusoidally varying strain or stress in time at a frequency ω. The corresponding stress or strain amplitudes are measured in time. The complex modulus G^* for a controlled strain experiment is determined as the ratio between the measured stress over the applied strain. The storage (elastic) modulus G' and the loss (viscous) modulus are deconvolved from G^*, considering the phase angle difference between the input strain wave and the resulting stress wave. A purely elastic stress response is in phase with the strain wave, and thus the phase angle is zero, whereas a purely viscous response is out of phase with the strain wave, and thus the phase angle is 90°. For a viscoelastic material, the phase angle lies somewhere between 0 and 90°. The corresponding expressions are $G' = G^*\cos\theta$ and $G'' = G^*\sin\theta$.

Thus, the expression relating the stress and strain during controlled strain dynamic testing is: $\tau = \gamma_0 G'\sin(\omega t) + \gamma_0 G''\cos(\omega t)$ where γ_0 is the maximum strain amplitude. Since during dynamic testing within small deformation, the microstructure of the fat crystal networks is unaffected, the G' represents the strength of the links between fat crystal clusters.

Small-deformation rheology experiments have been extensively used in the study on the viscoelastic properties of fat crystal networks. The rheological properties of a variety of model fat systems have been investigated by several groups (1,3,8,9,15,21,28,58–61). By combining rheology methods with various microscopy methods, attempts have been made to explain the change in the rheological properties of fat samples by a change in their microstructure. Nederveen (60) used a 20 to 30% tristearin suspension in liquid oil as a model fat system to study the relationship between the bending and torsion modulus and the SFC, the storage time, and the stress at varying frequencies. The bending and torsion moduli were found not to be dependent on frequency in the range of 40–1000 cps but increased considerably during storage. Heertje (21) studied the microstructure of shortenings before and after a compression experiment. The bridges between crystal clusters were found to be broken after compression, which implies that the intercrystal cluster links carry most of the stress during the deformation. Herrera and Hartel (35) reported that the compression storage modulus E' of a mixture of HMF and LMF is affected by crystallization temperatures and cooling rates.

Rousseau and Marangoni (61) measured the shear storage modulus G' and the shear loss modulus G'' of enzymatic interesterified and noninteresterified butter fat/canola oil blends by small-deformation rheology experiments. The difference in rheological properties of the enzymatic interesterified and noninteresterified butter fat/canola oil blends were closely related to the changes in their SFC and to a lesser extent to the distribution of solid crystal mass within the fat crystal networks. Marangoni and Rousseau (44) studied the hardness HI and the shear storage modulus G' of the chemically interesterified lard–canola oil (LCO) and palm oil–soybean oil (POSBO) blends ranging from 100% hardstock to 50%:50% hardstock/vegetable oil (w/w). The microstructure of the fat crystal networks in lard and palm oil was quantified rheologically using fractal dimensions. The different G' for interesterified and noninteresterified LCO and POSBO were non-SFC-related, since SFC of the samples did not change substantially with chemically interesterification. The spatial distribution of mass was not affected significantly either, since the microstructure of the fat crystal networks quantified by fractal dimensions did not change as well. The increased G' of chemically interesterified LCO was suggested to be related to the change in the properties of the particles that make up the network.

All of these studies implied that the rheological properties of fat crystal networks are the results of a combined effect of SFC, the microstructure of the fat crystal networks, and the properties of the particles making up the networks. Since the 1960s, different physical models of fat crystal networks have been proposed to quantitatively investigate the relationship between the physical properties of fats and their microstructure.

MODELS OF FAT CRYSTAL NETWORKS

Work on modeling of fat crystal networks started as early as the 1960s, when Van den Tempel proposed the linear chain model (1). In this model, solid fat particles are held together by two types of bonds—irreversible primary bonds and reversible secondary bonds—and form linear chains, which eventually form a fat crystal network. The primary bonds are stronger than the secondary bonds and may consist of relatively strong van der Waals forces. The breakage of strong irreversible primary bonds explained the work -softening phenomena of margarine and butter after kneading (21,59). In this model, the shear modulus G is predicted to be directly proportional to the volume fraction Φ of solids and to particle diameter D according to the equation:

$$G = 5A\,\Phi D^{0.5}/(24\pi H_0^{3.5}) \qquad [10]$$

where A is Hamaker's constant, H_0 is the interparticle distance, and Φ is the volume fraction of solids (usually determined as SFC/100). However, the experimental results (28,44,60–62) do not agree with the prediction; the G was observed to increase, not in a linear fashion with the volume fraction of solids, but rather in an exponential fashion. (6,62).

Sherman (6) proposed a different model that was similar to a flocculated oil-in-water emulsion. The fat crystal networks were described as less densely packed areas formed by the joining of localized regions of densely packed particles. However, Sherman's model still predicts a linear relationship between G and Φ, which is not supported by experiments. Realizing the stronger dependence of G on Φ and D than the prediction of the linear chain model, van den Tempel extended his model (15). The fat crystal network was still described as a network formed by linear chains, but the chains consisted of preformed aggregates instead of rigid sphere fat particles. The interaction between neighboring aggregates in a chain was proposed to be the sum of the interactions between the particles in contact between clusters. The tensile force in one principal direction was

related to the interaction between particles in contact. A correction factor was introduced into the calculation of the G of the fat crystal networks. The shear modulus G was recalculated as:

$$G = G_{theory} \bullet \frac{mD_a}{nD} \quad [11]$$

where G is the corrected shear modulus of the fat crystal network, G_{theory} is the shear modulus of the network calculated from the linear chain model, m is the number of connecting chains between two neighboring aggregates, n is the average number of primary particles in an aggregate, D_a is the average diameter of an aggregate, and D is the average primary particle diameter.

More realistic results were reported by fitting the experimental results (1,60) to the extended linear chain model. However, owing to the difficulties in calculating the correction factor and the lack of success of the previous linear chain model, this model has not been widely used.

Fractal geometry principles are now applied to quantitatively describe the structure of fat crystal networks (3,8). Fat crystal networks are modeled as cross-linked fractal clusters that are formed by the aggregation of fat crystals. On stressing the material, the links between the fractal fat crystal clusters carry most of the stress and are irreversibly broken when the deformation of the fat crystal networks is beyond its limit of linearity. A self-similar character is assumed to exist within the clusters, from primary fat crystals to the clusters. A theoretical schematic of the fat crystal networks under stress is shown in Figure 4 (45). If one were to express the force-constant of the links between microstructures as k_l, then the macroscopic elastic constant K (in one dimension) of the network could be written as:

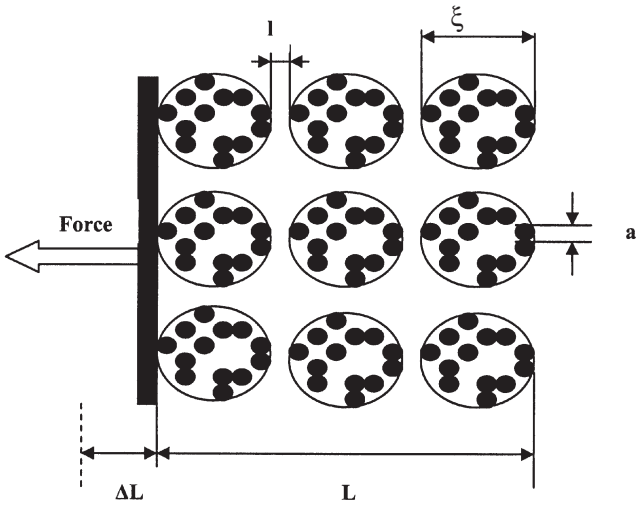

FIG. 4. Theoretical schematic of the fat crystal network under small deformation (45). a, diameter of one microstructure; L, microscopic size of the system; ΔL, change of the size of the system under external force; l, distance between two microstructures; ξ, diameter of a microstructural element.

$$K = [L/\xi]^{d-2} k_l \quad [12]$$

where ξ is the diameter of one microstructure, L is the macroscopic size of the system, and d is the Euclidean dimension of the sample ($d = 3$). Particles of diameter a are packed in a fractal fashion within flocs with size ξ. A force F acting on the network causes the links between flocs to yield, and the original length of the system in the direction of the applied force to change by ΔL. Thus, the interfloc separation distance l also changes. Since the structure within the microstructure is fractal in nature, the diameter of the microstructure (or aggregates) is related to the particle volume fraction of the fat crystal networks Φ as: $\xi \sim \Phi^{1/(D-3)}$. By substituting this expression into the expression of the macroscopic elastic constant of network K and assuming the links between the microstructures are statistically identical, then K is related to Φ as $K \sim \Phi^{1/(3-D)}$. Because the shear storage modulus of the network is related in a proportional manner to the force constant K, the G' is related to the particle volume fraction *via* the fractal dimension of the network as (3,9,11,45–47):

$$G' = \lambda \Phi^{\frac{1}{3-D}} \quad [13]$$

The fractal dimension D is used to quantify the microstructure of the fat crystal networks. The constant λ depends on the links between microstructures and the relationship between ξ, Φ, and D, as well as the nature of the proportionality between Φ (the SFC of the system) and Φ_l (the SFC within a cluster).

In practice, to measure the fractal dimensions of fat crystal networks, the shear modulus of the fat crystal networks G' within the LVR (linear viscoelastic region, where the stress increases with strain at a constant rate) is measured by small-deformation rheology experiments. By measuring the G' of fat crystal networks at different SFC, Φ, and plotting the logarithm of G' against logarithm of Φ, the fractal dimensions of the system can be determined from the slope of the curve as $D = 3 - 1/\text{slope}$.

Fractal analysis is a powerful tool for studying the microstructure of fat crystal networks. Vreeker *et al.* (8) used the fractal dimensions of tristearin aggregates to explain the power law relationship between the published G' and SFC data. In the determination of fractal dimensions by Vreeker *et al*. (8), the fat crystal networks were assumed to be in the strong link regime according to the theory of Shih *et al*. (63), in which $G' \sim \Phi^u$, and $u = (3 + x)/(3 - d)$, where d is the fractal dimension of the fat crystal network, and x is usually is in the range 1–1.3.

Marangoni and Rousseau (3) recognized that fat crystal networks at high SFC values are in the weak link regime, so they applied the weak-link theory of Shih *et al.* (63) to high-SFC systems and used fractal dimensions to quantify the microstructure of fat crystal networks. By assuming a spherical geometry for the microstructure elements, Narine and Marangoni (4) obtained an expression for the elastic modulus of a fat crystal network based on fractal scaling concepts:

$$G' = \frac{mA}{6c\pi a\xi d_0^3}\Phi^{\frac{1}{d-D}} \quad [14]$$

where m is the number of neighboring microstructural elements at the interface between two microstructures, A is the Hamaker's constant, c is a constant in the expression $N = cR^D$ (N is the number of primary particles in a cluster, R is the radius of the cluster, D is the mass fractal dimension of the cluster), a is the diameter of a microstructural element, ξ is the diameter of one microstructure, and d_0 is the average equilibrium distance between microstructural elements. In addition to the power law relationship $G' \sim \Phi^{1/(d-D)}$, Narine and Marangoni (4) explained the negative relationship between the hardness of fat samples and their particle size (6,60) by the cross-linked fractal clusters model of fat crystal networks.

The model of fat crystal networks was further developed by Marangoni through a thermodynamic approach (45). A general formulation for the relationship between the elastic modulus and the microstructure of high volume fraction aggregate networks has been obtained, namely,

$$E \sim \frac{12\left(\frac{\Delta U_\xi}{(l_0 - l)}\right)}{\pi a\xi\gamma}\Phi^{\frac{1}{d-D}} \quad [15]$$

where E is the Young's modulus of the fat crystal networks, ΔU_ξ corresponds to the change in internal energy per floc–floc bond, l_0 is the equilibrium distance between flocs, l corresponds to the distance between flocs under an applied stress, a is the diameter of the particles within the floc, ξ is the diameter of the flocs, γ is the strain of the network ($\gamma = \Delta L/L$, where ΔL is the deformation of the network and L is the size of the network), Φ is the volume fraction of the aggregate of the network, d is the Euclidean dimension of the space where the network is embedded, and D is the fractal dimension for the arrangement of particles within the network. By substituting ΔU_ξ for the interparticle interactions in a specific network, this extended model is suitable to study any soft materials network at high volume fractions. For example, by knowing that the interaction forces between the structural elements of a fat crystal network are van der Waals' forces, the Young's modulus of the fat crystal networks with differently shaped flocs can be derived separately.

The extended fat crystal network model has been used to investigate the yield stress of soft materials (47), where an expression of the yield stress of a network structured as a space-filling collection of fractal particle flocs was obtained as

$$\sigma^* \sim \frac{6\delta}{a}\Phi^{\frac{1}{d-D}} \quad [16]$$

where σ^* is the yield stress, δ is the solid-liquid surface energy (interfacial tension), a is the diameter of the microstructural element, Φ is the solids' volume fraction of the samples, d is the Euclidean dimension of the space where the network is embedded, and D is the fractal dimension of the networks. The yield stress as a function of solids volume fraction for blends of milk fat, cocoa butter, and modified palm oil has been studied by small-deformation rheology experiments. The results corresponded well with the model described by Equation 15.

Fractal dimension from oil permeability measurements. In the oil migration method, the permeability coefficient B is measured for fat samples at different SFC values. The fractal dimensions of the fat crystal networks can be calculated from the slope of the log-log plot of the permeability coefficient of the fat samples against their SFC. The permeability coefficient B is defined as "the rate of flow of water (liquid oil in our case) through a unit cross-sectional area under a unit hydraulic gradient at the prevailing temperature" (64). The permeability coefficient B is calculated from the volumetric flow rate Q according to Darcy's law:

$$Q = \frac{B * A_c}{\eta} * \frac{\Delta P}{L} \quad [17]$$

where A_c is the cross-sectional area through which flow takes place, η is the viscosity of the liquid oil in the fat sample, and ΔP is the pressure applied to the permeating oil over the distance L. In addition, the flux through one fractal structure element also can be described by Poiseuille's law as: $Q = \pi r^4 \Delta P/(8\eta L)$, where r is the inside radius of the element and the other symbols have the same meanings as that in Darcy's law. By combining Darcy's law and Poiseuille's law and applying fractal geometry principles, Bremer *et al.* (24) showed that the permeability coefficient B is related to network structure as

$$B = \left(\frac{a^2}{M}\right)\Phi^{\frac{2}{D-3}} \quad [18]$$

where a is the particle size, M is a parameter similar to the tortuosity factor in the Kozeny-Carman equation (65), Φ is the solid's volume fraction, and D is the fractal dimension of the network. Combining these two equations, D is related to Q as

$$Q = \left(\frac{A_c}{\eta} * \frac{\Delta P}{L}\right) * \left(\frac{a^2}{K}\right) * \Phi^{\frac{2}{D\text{-}3}} \quad [19]$$

Thus, the fractal dimensions D can be calculated from the volumetric flow rate Q data at different solids volume fraction, Φ. Dibildox-Alvarado *et al*. (66) applied the equation of Bremer *et al.* to analyze the oil migration data for mixtures of peanut oil and IHPO (chemically Interesterified and Hydrogenated Palm Oil) cooled at different cooling rates. Dibildox-Alvarado *et al*. (66) measured the D_b and D_f of the fat samples and successfully predicted the increased permeability coefficient at a lower cooling rate according to Equation 18 of Bremer *et al*. (24). Tang and Marangoni (67) studied the microstructure of the mixture of tristearin and sunflower oil using the oil migration method. Higher fractal dimensions were found for the samples cooled at higher cooling rates. A good fit ($r^2 = 0.99$) was found for the nonlinear regression of the equation of Bremer *et al*. to the data as seen in Figure 5.

Fractal dimensions by light scattering. In addition to the rheology method and the permeability coefficient method, the fractal dimensions of fat crystal networks can also be obtained using light scattering. When light travels through a dilute sus-

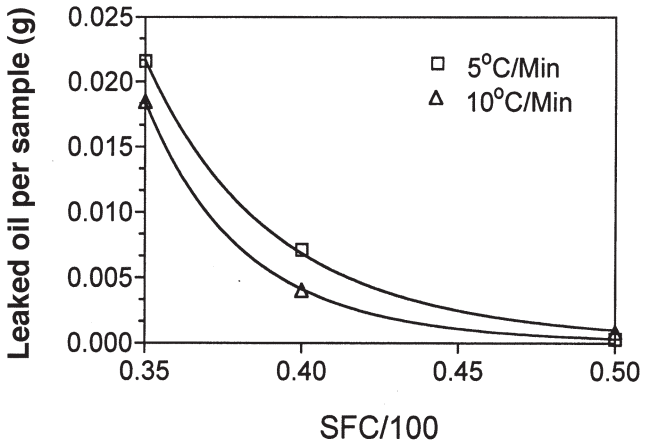

FIG. 5. Nonlinear regression curves of oil migration data. SFC, solid fat content.

pension of fat crystals in oil, it will be scattered by the crystallites. The intensity of the scattering is generally considered to be a function of two components, $S(q)$, which is the structure factor corresponding to the scattering due to the spatial correlation between particles, and $P(q)$, which is the form factor corresponding to the scattering arising from the properties of individual particles. The scattering intensity $I(q)$ is thus a product of the structure factor and the form factor, namely, $I(q) \sim S(q)*P(q)$. At small values of the scattering vector **q**, $P(q)$ is considered to be a constant, so the variation of the scattering intensity mainly comes from the spatial distribution of the fat clusters in the fat crystal networks, which is expressed as: $I(q) \sim q^{-D}$. The scattering vector has the following form: $\mathbf{q} = (4\pi/\lambda) \sin(\theta/2)$, where λ is the wavelength of the light and θ is the scattering angle. The light scattering fractal dimension D is calculated as the negative of the slope of the log-log plot of the scattering intensity I(q) with the scattering vector **q** (8). This equation is only valid when **q** is within the range: $1/R_g << \mathbf{q} << 1/r_0$, where R_g is the size of the aggregate and r_0 is the size of the primary particle. The light-scattering technique has been used to study the microstructure of fat crystal networks. Vreeker *et al.* (8) studied the change in microstructure of a dispersion of glycerol tristearate in olive oil during storage after rapid cooling from 90 to 2°C. The fractal dimensions of the samples from the light-scattering method increased from 1.7 to 2.0 after 7 d of storage. More compact fat crystal clusters were related to the increased fractal dimension. The fractal dimensions calculated using the rheology method was 2.0, corresponding well with the fractal dimensions from the light-scattering method. For application of the light-scattering method, the samples have to be optically transparent, so this method is useful only for fats with very low SFC.

SUMMARY AND FUTURE WORK

In food products, fat is structured macroscopically as fat crystal networks, with a different structure at different length scales. The microstructure of fat crystal networks including the morphology and spatial distribution of the fat crystal clusters is the determining factor of the rheology and other physical properties in these materials. Among the physical models used to describe the microstructure of fats, the fractal model best describes the observed behavior. However, the physical meaning of the various fractal dimensions used in the quantification of structure remains unclear. It is necessary to study the determining factors of these fractal dimensions to explore their physical basis experimentally and in theory in order to explain the behavior of the physical properties of fats. In addition, the ability to quantify the microstructure of fat crystal networks using other structural parameters needs to be evaluated and compared with the fractal dimensions.

REFERENCES

1. Van den Tempel, M., Mechanical Properties of Plastic Disperse Systems at Very Small Deformation, *J. Colloid Sci. 16*:284–296 (1961).
2. de Man, J.M., Microscopy in the Study of Fats and Emulsions, *Food Microstruct. 1*:209–212 (1982).
3. Marangoni, A.G., and D. Rousseau, Is Plastic Fat Rheology Governed by the Fractal Geometry of the Fat Crystal Network? *J. Am. Oil Chem. Soc. 73*:991–994 (1996).
4. Narine, S.S., and A.G. Marangoni, Fractal Nature of Fat Crystal Networks, *Phys. Rev. E 59*:1908–1920 (1999).
5. Marangoni, A.G., The Nature of Fractality in Fat Crystal Networks, *Trends Food Sci. Technol. 13*:37–47 (2002).
6. Sherman, P., The Influence of Particle Size on the Viscoelastic Properties of Flocculated Emulsions, *5th International Conference on Rheology*, Kyoto, Japan, 1968, pp. 327–338.
7. Haighton, A.J., Measurement of the Hardness of Margarines and Fats with the Cone Penetrometer, *J. Am. Oil Chem. Soc. 36*:345–348 (1959).
8. Vreeker, R., L.L. Hoekstra, D.C. den Boer, and W.G.M. Agtero, The Fractal Nature of Fat Crystal Networks, *Colloids Surf. 65*:185–189 (1992).
9. Narine, S.S., and A.G. Marangoni, Mechanical and Structural Model of Fractal Networks of Fat Crystals at Low Deformation, *Phys. Rev. E 60*:6991–7000 (1999).
10. Marangoni, A.G., The Nature of Fractility in Fat Crystal Networks, in *Fat Crystal Networks*, edited by A.G. Marangoni, Marcel Dekker, New York, 2005, pp. 413–440.
11. Narine, S.S., and A.G. Marangoni, Microstructure, *Ibid.*, pp. 179–255.
12. Rousseau, D., A.R. Hill, and A.G. Marangoni, Restructuring Butterfat Through Blending and Chemical Interestification. 2. Microstructure and Polymorphism, *J. Am. Oil Chem. Soc. 73*:973–981 (1996).
13. Awad, T.S., M.A. Rogers, and A.G. Marangoni, Scaling Behavior of the Elastic Modulus in Colloidal Networks of Fat Crystals, *J. Phys. Chem. B 108*:171–179 (2004).
14. Campos, R., S.S. Narine, and A.G. Marangoni, Effect of Cooling Rate on the Structure and Mechanical Properties of Milk Fat and Lard, *Food Res. Int. 35*:971–981 (2002).
15. Van den Tempel, M., Rheology of Concentrated Suspensions, *J. Colloid Interface Sci. 71*:18–20 (1979).
16. Shi Y., B. Liang, and R.W. Hartel, Crystal Morphology, Microstructure, and Textural Properties of Model Lipid Systems, *J. Am. Oil Chem. Soc. 82*:399–408 (2005)
17. Heertje, I., M. Leunis, W.J.M. van Zeyl, and E. Berends, Product Morphology of Fatty Products, *Food Microstruct. 6*:1–8 (1987).
18. Manning, D.M., and P.S. Dimick, Crystal Morphology of Cocoa Butter, *Ibid. 4*:249–265 (1985).

19. Litwinenko, J.W., Fat Crystal Network Microstructure Image Archive DVD, accompaniment to *Fat Crystal Networks*, edited by A.G. Marangoni, Marcel Dekker, New York, 2005.
20. Herrera, M.L., and R.W. Hartel, Effect of Processing Conditions on Physical Properties of a Milk Fat Model System: Microstructure, *J. Am. Oil Chem. Soc. 77*:1197–1204 (2000).
21. Heertje, I., Microstructure Studies in Fat Research, *Food Microstruct. 12*:77–94 (1993).
22. Juriaanse, A.C., and I. Heertje, Microstructure of Shortenings, Margarine and Butter—A Review, *Ibid. 7*:181–188 (1988).
23. Heertje, I., V. Eendenburg, J.M. Cornelissen, and A.C. Juriaanse, The Effect of Processing on Some Microstructural Characteristics of Fat Spreads, *Ibid. 7*:189–193 (1988).
24. Bremer, L.G.B., T.V. Vliet, and P. Walstra, Theoretical and Experimental Study on the Fractal Nature of the Structure of Casein Gels, *J. Chem. Soc., Faraday Trans. I, 85*:3359–3372 (1989).
25. Marangoni, A.G., Crystallization Kinetics, in *Fat Crystal Networks*, edited by A.G. Marangoni, Marcel Dekker, New York, 2005, pp. 56–60.
26. Litwinenko, J.W., Imaging of a Model Plastic Fat System by 3-Dimensional Wide-Field Transmitted Polarized Light Microscopy and Image Deconvolution, *Ibid*., pp. 711–829.
27. Jewell, G.G., and M.L. Meara, A New and Rapid Method for the Electron Microscopy Examination of Fats, *J. Am. Oil Chem. Soc. 47*:535–538 (1970).
28. de Man, J.M., and A.M. Beers, Fat Crystal Networks: Structure and Rheological Properties, *J. Texture Stud. 18*:303–318 (1987).
29. Martini, S., M.L. Herrera, and R.W. Hartel, Effect of Processing Conditions on Microstructure of Milk Fat Fraction/Sunflower Oil Blends, *J. Am. Oil Chem. Soc. 79*:1063–1068 (2002).
30. Singh A.P., C. Bertoli, P.R. Rousseau, and A.G. Marangoni, Matching Avrami Indices Achieves Similar Hardnesses in Palm Oil-Based Fats, *J. Agric. Food Chem. 52*:1551–1557 (2004).
31. Mazzanti, G., S.E. Guthrie, E.B. Sirota, A.G. Marangoni, and S.H.J. Idziak, Orientation and Phase Transitions of Fat Crystals Undershear, *Cryst. Growth Des. 3*:721–725 (2003).
32. Mazzanti, G., A.G. Marangoni, S.H.J. Idziak, Modeling Phase Transitions During the Crystallization of a Multicomponent Fat Under Shear, *Physical Review E 71*:041607 (2005).
33. Failey, P., J.M. Krochta, and J.B. German, Crystal Morphology of Mixtures of Tripalmitin and Butterfat, *J. Am. Oil Chem. Soc. 72*:693–697 (1995).
34. Herrera, M.L., and R.W. Hartel, Effect of Processing Conditions on Crystallization Kinetics of a Milk Fat Model System, *Ibid. 77*:1177–1187 (2000).
35. Herrera, M.L., and R.W. Hartel, Effect of Processing Conditions on Physical Properties of a Milk Fat Model System: Rheology, *Ibid. 77*:1183–1195 (2000).
36. Walstra, P., *Physical Chemistry of Foods*, Marcel Dekker, New York, 2003, pp. 302–306.
37. Mandelbrot, B.B., *The Fractal Geometry of Nature*, Freeman, New York, 2005.
38. Avnir, D., D. Farin, and P. Pfeifer, Surface Geometric Irregularity of Particulate Materials: The Fractal Approach, *J. Colloid Interface Sci. 103*:112–123 (1985).
39. Awad, T.S., and A.G. Marangoni, Comparison Between Image Analysis Methods for the Determination of the Fractal Dimensions of Fat Crystal Networks, in *Fat Crystal Networks*, edited by A.G. Marangoni, Marcel Dekker, New York, 2005, pp. 391–399.
40. Russ, J.C., *Fractal Surfaces*, Plenum Press, New York, 1994, pp. 98–101.
41. Tang, D., and A.G. Marangoni, Computer Simulation of Fractal Dimension of Fat Crystal Networks, *J. Am. Oil Chem. Soc. 83:*309–314 (2006).
42. Marangoni, A.G., and S.E. McGauley, Relationship Between Crystallization Behavior and Structure in Cocoa Butter, *Cryst. Growth Des. 3*:95–108 (2003).
43. Batte, H.D., and A.G. Marangoni, Fractal Growth of Milk Fat Crystals Is Unaffected by Microstructural Confinement, *Ibid. 5*:1703–1705 (2005).
44. Marangoni, A.G., and D. Rousseau, The Influence of Chemical Interesterification on the Physicochemical Properties of Complex Fat System. 3. Rheology and Fractality of the Crystal Network, *J. Am. Oil Chem. Soc. 75*:1633–1636 (1998).
45. Marangoni, A.G., Elasticity of High-Volume-Fraction Aggregate Networks: A Thermodynamic Approach, *Phys. Rev. B 62*:13951–13955 (2000).
46. Narine, S.S., and A.G. Marangoni, Relating Structure of Fat Crystal Networks to Mechanical Properties: A Review, *Food Res. Int. 32*:227–248 (1999).
47. Marangoni, A.G., and M.A. Rogers, Structural Basis for the Yield Stress in Plastic Disperse Systems, *Appl. Phys. Lett. 82*:3239–3241 (2003).
48. Litwinenko, J.W., A.P. Singh, and A.G. Marangoni, Effects of Glycerol and Tween 60 on the Crystallization Behavior, Mechanical Properties, and Microstructure of a Plastic Fat, *Cryst. Growth Des. 4*:161–168 (2004).
49. Huang, Y.B., and P. Somasundaran, Effects of Random Walk Size on the Structure of Diffusion-Limited Aggregates, *Phys. Rev. A 36*:4518–4521 (1987).
50. Wu, Z., and B. Li, Random Success Growth Model for Pattern Formation, *Phys. Rev. E 51*:16–19 (1995).
51. AOCS, *Official Methods and Recommended Practices of the AOCS*, 5th ed., AOCS Press, Champaign, 1997.
52. Rebinder, P.A., and N.A. Semanenko, Use of the Penetrating Cone Method for the Characterization of Structural-Mechanical Properties of Visco-plastic Material, *Proc. Acad. Sci. (U.S.S.R.) 64*:835–838 (1949).
53. Mottram, F.J., Evaluation of Pseudo-plastic Materials by Cone Penetrometers, *Lab. Pract. 10*:767–770 (1961).
54. Vasic, I., and J.M. de Man, Effect of Mechanical Treatment on Some Rheological Properties of Butter, in *Rheology and Texture of Food Stuffs*, Society of Chemical Industry, London, 1968, Monograph 27, pp. 251–264.
55. Dixon, B.D., and J.V. Parekh, Use of the Cone Penetrometer for Testing Firmness of Butter, *J. Texture Stud. 10*:421–434 (1979).
56. Hayakawa, M., and J.M. Man, Interpretation of Cone Penetrometer Consistency Measurements of Fats, *Ibid. 13*:201–210 (1982).
57. Rousseau, D., and Marangoni, A.G., The Effects of Interesterification on Physical and Sensory Attributes of Butterfat and Butterfat–Canola Oil Spreads, *Food Res. Int. 31*:381–388 (1999).
58. Liang, B., and R.W. Hartel, Effects of Milk Powders in Milk Chocolate, *J. Dairy Sci. 87*:20–31 (2004).
59. Wright, A.J., M.G. Scanlon, R.W. Hartel, and A.G. Marangoni, Rheological Properties of Milk Fat and Butter, *J. Food Sci. 66*:1056–1071 (2001).
60. Nederveen, C.J., Dynamic Mechanical Behavior of Suspensions of Fat Particles in Oil, *J. Colloid Sci. 18*:276–291 (1963).
61. Rousseau, D., and A.G. Marangoni, Tailoring the Textural Attributes of Butter Fat/Canola Oil Blends *via Rhizopus arrhizus* Lipase-Catalyzed Interesterification. 2. Modification of Physical Properties, *J. Agric. Food Chem. 46*:2375–2381 (1998).
62. Payne, A.R., The Elasticity of Carbon Black Networks, *J. Colloid Sci. 19*:744–754 (1964).
63. Shih., W.H., W.Y. Shih., S.I. Kim, J. Liu., and I.A. Aksay, Scaling Behavior of the Elastic Properties of Colloidal Gels, *Phys. Rev. A 42*:4772–4779 (1990).
64. ASCE (American Society of Civil Engineers), Manual 40–Ground Water Management, 1985. Netlink: http://or.water.usgs.gov/projs_dir/willgw/glossary.html#p (accessed June 2005).
65. Davies, L., and D. Dollimore, Theoretical and Experimental

Values for the Parameter *k* of the Kozeny–Carman Equation, as Applied to Sedimenting Suspensions, *J. Phys. D: Appl. Phys. 13*:2013–2020 (1980).
66. Dibildox-Alvarado, E., J.N. Rodrigues, L.A. Gioielli, J.F. Toro Vazquez, and A.G. Marangoni, Effects of Crystalline Microstructure on Oil Migration in a Semisolid Fat Matrix, *Cryst. Growth Des. 4*:731–736 (2004).
67. Tang, D., and A.G. Marangoni, Quantitative Measurement of Microstructure of Fat Crystal Networks by Microscopy and Rheology Methods, presented at the 96th AOCS Annual Meeting and Expo, Salt Lake City, May 2005.

[Received September 14, 2005; accepted February 6, 2006]